AIAA JOURNAL
Vol. 30, No. 6, June 1992

# Acoustic Sources in a Tripped Flow past a Resonator Tube

M. C. Thompson,* K. Hourigan,† and M. C. Welsh‡
*Commonwealth Scientific and Industrial Research Organisation, Highett, Victoria 3190, Australia*
and
E. Brocher§
*Université d'Aix-Marseille, 13003 Marseille, France*

**A numerical model employing the vortex method is used to investigate the separated flow around a trip rod placed upstream of a resonator tube. The acoustic power generated by the flow is calculated using Howe's theory of aerodynamic sound. When the trip rod is placed far enough upstream, natural vortex shedding from the rod proceeds and no net acoustic energy of the tube resonant mode is generated. However, when the rod is placed close to the tube, the vortex shedding becomes locked to the acoustic field, changes to a symmetric mode, and the flow generates net resonant acoustic energy per acoustic cycle. These results are consistent with previous experimental observations and provide insight into the flow structures responsible for the transfer of energy from the flowfield to the resonant acoustic field.**



## Nomenclature

$B$ = stagnation enthalpy
$b$ = dimension of leading edge of trip rod
$c$ = speed of sound
$d$ = spacing between trip rod and resonator tube on axis of symmetry
$Fr$ = Froude number, $\equiv v_\infty/\sqrt{g\bar{h}}$
$f$ = sound frequency
$G(.)$ = function transforming from $z$ to $\zeta$ plane
$g$ = standard gravity
$h$ = water height in hydraulic analogy
$\bar{h}$ = mean water height in hydraulic analogy
$i$ = $\sqrt{-1}$
$K(.,.)$ = coupling coefficient
$k$ = unit vector
$L(.,.)$ = coupling coefficient
$M$ = Mach number
$P$ = acoustic power
$P_{ref}$ = reference rate of energy flow into tube
$p$ = acoustic pressure
$St_a$ = acoustic Strouhal number, $\equiv fb/v_\infty$
$s$ = surface coordinate
$T$ = acoustic period
$u$ = acoustic particle velocity
$u_{mouth}$ = spatial average acoustic particle velocity amplitude at the mouth of the tube
$V$ = complex velocity
$V_{irr}$ = complex irrotational velocity
$V_{wedge}$ = correction to the complex velocity due to the presence of the wedge
$v$ = flow velocity
$v_{irr}$ = irrotational component of flow velocity
$v_t(s)$ = tangential surface velocity at complex position $s$
$v_{wedge}$ = velocity correction due to the wedge
$v_\infty$ = flow velocity at upstream infinity
$W$ = width of resonator tube opening
$x,y$ = physical Cartesian coordinates
$Y$ = complex velocity
$z$ = complex coordinate in physical plane, $\equiv x + iy$
$\alpha$ = level of resonant acoustic amplitude
$\Gamma$ = circulation
$\gamma$ = ratio of specific heats
$\Delta h_{max}$ = theoretical maximum water height oscillation, $2Fr\,\bar{h}$
$\lambda$ = wavelength of resonant sound
$\xi,\eta$ = transformed coordinates in complex plane
$\rho_0$ = mean fluid density
$\sigma$ = vorticity density
$\tau$ = time
$\phi$ = acoustic pressure amplitude
$\omega$ = vorticity

Received Jan. 4, 1991; revision received Aug. 29, 1991; accepted for publication Sept. 10, 1991. 

*Senior Research Scientist, Division of Building, Construction, and Engineering, P.O. Box 56.
†Principal Research Scientist, Division of Building, Construction, and Engineering, P.O. Box 56.
‡Senior Principal Research Scientist, Division of Building, Construction, and Engineering, P.O. Box 56.
§Research Director 1, Institut de Mécanique des Fluides, Unité Mixte 34 of the Centre National de la Recherche Scientifique, 1, rue Honnorat.

## Introduction

THE interaction of acoustic fields with flowfields has recently been the subject of numerous investigations.[1-3] It has been found that certain flow configurations lead to strong coupling of the two fields. In typical situations, vortex shedding from one or more bodies may be locked in frequency to the resonant acoustic field and in turn this periodic vortex shedding may feed energy into the acoustic field, resulting in positive feedback and resonance.

An understanding of the generation of acoustic power by vortices traveling through acoustic fields has come through the application of Howe's[4,5] theory of aerodynamic sound and discrete vortex models of the flow. Welsh et al.[2] examined the fluid mechanics of the resonant process in a duct containing a plate with semicircular leading edges. The resonant process is described in terms of an interchange of energy between the flow and acoustic fields and has three basic components: 1) a sound source (the vortex street), 2) a feedback effect of the sound on the vortex shedding, and 3) a damping process whereby acoustic energy is transferred out of the duct system. Similarly, a study of the acoustic resonant process and the mechanism coupling the vortex shedding and the acoustic field was investigated for tandem plates in a duct flow by Stoneman et al.[6]

Vrebalovich[7] has shown experimentally that it is possible to generate strong oscillations within a tube placed in a supersonic flow by locating triggering devices upstream of the tube mouth. Brocher[8] and Brocher and Duport[9] extended Vreba-

Sprenger tube.[11] This maximum amplitude is obtained from the relation given in Brocher and Duport,[9] which can be linearized to $\Delta p_{\max} \simeq 2\gamma M p_a$, where $\gamma$ represents the ratio of specific heats and $p_a$ is the ambient pressure. This relation can be derived from linear acoustic theory by imposing a velocity amplitude at the tube mouth equal to the freestream velocity $v_\infty$. This means that, when the limit cycle is achieved, the flow is largely absorbed by the tube during the inflow phase.

The role of the vortex shedding from the triangular cross-sectioned trip rod in exciting the tube acoustic resonance was elucidated through flow visualization by Kawahashi et al.[12] using a free surface hydraulic analogy. It was found that when strong oscillations within the tube were excited, the vortex shedding from the trip rod changed from being asymmetrical (natural) to symmetrical. The vortex shedding was locked to the oscillation within the tube, indicating that the vortex shedding plays an important role in stimulating growth and sustaining resonant oscillations within the tube. For some configurations, Kawahashi et al.[12] found water level fluctuations $\Delta h$ that approached the value given for the limit cycle of Hartmann-Sprenger tubes, which in the case of the hydraulic analogy is $\Delta h_{\max} = 2Fr\bar{h}$, where $Fr$ is the Froude number and $\bar{h}$ is the mean water height.

The present paper investigates the vortex shedding from a wedge-shaped trip rod in a flow past a resonator tube in terms of Howe's theory of aerodynamic sound. In particular, an understanding of the phase relationship between the vortex shedding and the resonant acoustic field, and spatial and temporal details of the acoustic source regions, are sought for low Mach number flows. A vortex model simulates the shedding of vortex clouds from the trip rod and their passage past the resonator tube, showing how the large-scale vortex shedding rate can become locked to the sound frequency and predicting the generation of acoustic power. It should be noted that this study concentrates on the sound sources and flow description when the acoustic resonance in the tube has attained the equilibrium state. The equilibrium state is a limit cycle that appears experimentally to be insensitive to the initial conditions. No attempt is made to analyze the complex transient excitation of the acoustic resonance and the initial appearance and Gerrard-Bloor amplification of linear disturbances in the flow. In the equilibrium state, the forcing of the flow around a bluff body by the feedback of loud resonant sound results in the growth of disturbances in the separating shear layers at the forcing frequency to nonlinear levels without requiring Gerrard-Bloor amplification. This is termed a high-intensity bypass by Morkovin,[13] whereby the system can no longer be considered linear for large excursions from the unperturbed state and the periodic forcing can dominate over transient responses growing exponentially in time. This type of response to forcing has been observed recently by Tokumaru and Dimotakis[14] for a circular cylinder.

## Mathematical Modeling of the Feedback Process

The current investigation of the resonant feedback process does not involve a direct simulation of the development and interaction of the resonant acoustic field and the flowfield. With currently available resources, such a simulation would be computationally very expensive due to at least two factors. First, the acoustic time scale is much smaller than the dynamic (flow) time scale at low Mach numbers. Thus, a very small time step (relative to the dynamic time scale) is required to accurately model acoustic wave motions. Second, resonances can build up very slowly over many acoustic cycles, hence, very long integration times (i.e., many time steps) and an accurate treatment of wave reflection and transmission at boundaries are required. Consequently, a simpler model, which does not attempt to model the transient stage over which the resonance builds up, has been used to provide some insight into the physics underpinning the resonance process.

For this model, it is assumed that the (resonant) acoustic field exists and is in equilibrium, as observed in practice by Kawahashi et al.[12] after the initial excitation stage. The flowfield is modeled using the discrete vortex method, which has been found to accurately model the large-scale vortex structures especially when strong forcing locks the shedding. The energy transfer from the flow to the acoustic field is then investigated using a theory due to Howe[4,5] which relates the rate of change of acoustic energy to the existing flow (vortical plus potential) and sound field. The amplitude of the resonant acoustic field is taken to be constant over the acoustic cycle when the system has reached equilibrium. This assumption is justified on the basis that only a small amount of energy, relative to the energy residing in the high-amplitude resonant acoustic field, is transferred each acoustic cycle between the flow and acoustic field due to the vortex shedding from the wedge. At equilibrium, an equal amount of energy is removed from the resonant acoustic field by radiation and other damping losses.

If the acoustic power density integrated over time and space (i.e., the energy transferred from the flow to the acoustic field) is significantly positive (that is, sufficient to balance acoustic energy losses due to radiation and damping), then it can be assumed that the resonance can be maintained. On the other hand, if the energy transferred is negative or not sufficient to overcome losses due to other mechanisms, then the assumed acoustic resonance would be deemed to be not sustainable. Furthermore, the time-integrated and instantaneous spatial distributions of acoustic power density show the positions of source or sink regions, and the instantaneous spatially integrated acoustic power density reveals the instantaneous direction of energy transfer.

For the numerical experiments, the tube and rod geometries are based on the experiments of Kawahashi et al.[12] Figure 1 shows a schematic of the geometry of the resonator tube with the trip rod placed upstream symmetrically about the centerline of the tube.

### Resonant Acoustic Field and Irrotational Flow

The acoustic mode to be modeled is a standing wave corresponding to an organ pipe mode of the tube. In the flows of interest, the Mach number is small and the acoustic pressure $p$ satisfies the wave equation:

$$\frac{\partial^2 p}{\partial \tau^2} = c^2 \nabla^2 p \tag{1}$$

where $c$ denotes the velocity of sound and $\tau$ is time.

The time-independent amplitude function $\phi$ can be extracted from a standing wave solution $p = \phi e^{i2\pi f\tau}$, where $f$ is the frequency. Then $\phi$ satisfies the Helmholtz equation:

$$\nabla^2\phi + (2\pi f/c)^2\phi = 0 \tag{2}$$

For the low-frequency modes, which are symmetrical about the longitudinal midplane, the following boundary condition applies on the rigid surfaces:

$$\boldsymbol{k} \cdot \nabla\phi = 0 \tag{3}$$

where $\boldsymbol{k}$ is the unit vector normal to the surface.

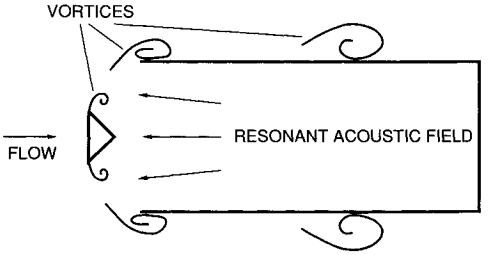


**Fig. 1 Schematic of resonator tube and trip rod (not to scale).**

Attention is focused on the region close to the trip rod and the tube opening where the shed vortices can do work on the sound field. The resonant mode of the tube of interest has a wavelength approximately four times the length of the tube, which in turn is much greater than the size of the vortex shedding region. Therefore, the spatial dependence of the sound field is approximated well in this vicinity by the solution of the Laplace equation. This can be seen from a simple scale analysis. The ratio of the second term to the first term of Eq. (2) is $(2\pi W/\lambda)^2$, where $\lambda$ is the wavelength of the tube resonant mode, and the tube half width $W/2$ is the characteristic length of spatial variation near the tube mouth. In the case being modeled, this ratio is of order $10^{-2}$. That is, Eq. (2) can be reasonably approximated near the tube mouth by $\nabla^2\phi = 0$, and the velocity oscillations near the tube mouth due to the sound field are obtained by assuming the tube to be semi-infinite with a sinusoidally oscillating potential flow source at downstream infinity.

The potential flow solution for the oscillating flow is obtained using a Schwarz-Christoffel transformation to project the real plane containing a semi-infinite tube into the upper half-plane with the boundary of the tube along the real axis (Fig. 2). The transformation from the physical ($z$) plane to the transformed ($\zeta$) plane that maps the leading tip corners of the tube $z = \pm iW/2$ into the points $\zeta = \pm 1$ is given by

$$z = \frac{W}{\pi}\left(\frac{\zeta^2}{2} - \log\zeta\right) + (W/2)\left(i - \frac{1}{\pi}\right) \tag{4}$$

where $i = \sqrt{-1}$. The irrotational flow velocity representing flow into and out of the tube, and therefore approximating the sound field, is then given by

$$v_{\text{irr}} = [v_{\text{irr},x},\ v_{\text{irr},y}] = [\text{real}(V_{\text{irr}}),\ \text{imag}(V_{\text{irr}})] \tag{5}$$

where

$$\frac{V_{\text{irr}}}{v_\infty} = 1 + \frac{1}{(\zeta^2 - 1)^*}(1 + \alpha \sin 2\pi f\tau) \tag{6}$$

Here, * denotes complex conjugate. The first term on the right-hand side of Eq. (6) represents the longitudinal irrotational flow from upstream infinity. The first part of the second term in parentheses represents the blockage effect of the tube, resulting in zero time-mean flow into the tube. The second part of the term in parentheses models the velocity near the tube opening due to the acoustic oscillations in the resonator tube. The parameter $\alpha$ lies in the range [0,1] and is a measure of the amplitude of the acoustic resonance. For example, when $\alpha = 1$, the amplitude of the oscillating potential flow source is equal to the freestream velocity $v_\infty$.

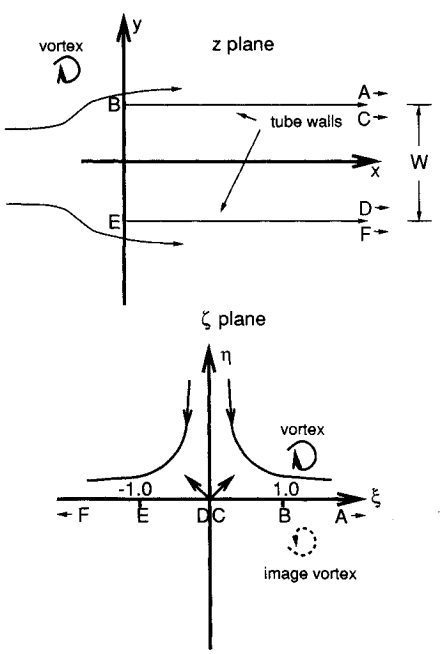


**Fig. 2 Schwarz-Christoffel mapping from physical $z$ plane to the transformed $\zeta$ plane.**

The modification to the potential flowfield (6) due to the presence of the trip rod can be taken account of approximately by applying the surface vorticity method described below. Point vortices can be placed around the surface of the wedge in the $\zeta$ plane, together with their images (in order to satisfy the zero normal flow at the tube walls), and the velocity field can then be calculated by transforming back to the real plane. The corrected velocity field is then given by

$$V = (V_{\text{irr}} + V_{\text{wedge}})$$

where

$$V^*_{\text{wedge}} = \sum_{n=1}^{N_{\text{wedge}}} \left\{\frac{i\Gamma_n}{2\pi}\left[\frac{1}{(\zeta - \zeta_n)} - \frac{1}{(\zeta - \zeta^*_n)}\right]\right\}\frac{d\zeta}{dz} \tag{7}$$

where the number of surface vortices $N_{\text{wedge}}$ and the strengths $\Gamma_n$ are determined by the method described in the following.

### Flow Modeling

The flow is modeled by a two-dimensional inviscid incompressible flow, irrotational everywhere except at the centers of elemental vortices. The shedding of vorticity is currently only allowed from the wedge and is modeled by the creation of the elemental vortices at the surface, to enforce the no-slip condition there. These elemental vortices are convected under the influence of other elemental vortices and the irrotational flow. The irrotational flow, which is the solution of the Laplace equation, is calculated using the Schwarz-Christoffel transformation (4). For the tube, the condition of zero normal flux is satisfied by positioning, for each elemental vortex in the flow, an image vortex of opposite signed circulation at the complex conjugate position in the transformed ($\zeta$) plane.

The effect of the trip rod on the flow is modeled using the surface vorticity method (see, e.g., Refs. 6 and 15), which imposes a no-slip condition at the surface. In brief, this method requires that the contour along the body surface is a streamline and that the tangential velocity on the inside of the vortex sheet is zero. Denoting the distance along the body surface in the $\zeta$ plane by $s$, discretization of a vortex sheet into $M$ segments, with the $n$th segment having length $\Delta s_n$ and linear vorticity density $\sigma(s_n)$, produces a set of linear equations:

$$\sum_{n=1}^{M} \sigma(s_n)K(s_n, s_m)\Delta s_n - \frac{1}{2}\sigma(s_m) = -v_t(s_m) - \sum_{n=1}^{N_v} \Gamma_n L(n, s_m), \qquad (m = 1, M) \tag{8}$$

where the last term gives the contribution to the velocity field at the surface due to $N_v$ free vortices and their images of circulation $\Gamma$ in the flow. The coupling coefficient $K(s_n, s_m)$ has the value of the surface tangential velocity at $s_m$ induced by a vortex of unit circulation at $s_n$ and an image vortex at $s^*_n$ of opposite circulation. The coupling coefficient $L(n, s_m)$ has the value of the surface tangential velocity at $s_m$ due to a vortex of unit circulation at the position of the $n$th free vortex and an image vortex of negative unit circulation at the conjugate position. The velocity $v_t(s_m)$ is the tangential velocity at surface position $s_m$ due to the background irrotational flow; that is, the tangential velocity component from Eq. (5). The solution of Eq. (8) gives the surface vorticity density at the pivotal points on the surface of the body, which are taken to be the center of each discrete element.

At each time step, the elemental vortices are created possessing the circulation of each vortex segment on the surface of the trip rod; vortices on the surface of the trip rod are released into the flow normal to the surface at half the corresponding vortex segment length to simulate the formation of the boundary layers. The zero normal flow condition on the surface of the resonator tube is effected through the introduction of image vortices at the corresponding conjugate positions in the $\zeta$ plane. The velocity at the center of vortex $j$ in the $z$ plane is given by

$$v_j = v_{\text{irr}} + v_{\text{wedge}} + [\text{real}(Y_j), \text{imag}(Y_j)] \tag{9}$$

where

$$\frac{Y_j}{v_\infty} = [g'(z_j)]^* \left\{ \sum_{\substack{n=1 \\ n \neq j}}^{N} \frac{i\Gamma_n}{2\pi} \left[ \frac{1}{(\zeta_j - \zeta_n)^*} - \frac{1}{(\zeta_j - \zeta_n^*)^*} \right] \right\} + \frac{i\Gamma_j}{4\pi} \left[ \frac{g''(z_j)}{g'(z_j)} \right]^* \tag{10}$$

Here, $\zeta = g(z)$ and $' \equiv \mathrm{d}/\mathrm{d}z$. The last term on the right-hand side is the Routh correction due to the transformation between planes.

The elemental vortices are potential vortices with smoothed cores (Rankine profile) of radius $0.03b$, where $b$ is the dimension of the leading edge of the triangular trip rod. Test cases with larger and smaller smoothing cores showed that the formation of the large-scale vortex structures and the acoustic power predictions were insensitive to the exact smoothing value used. The vortices are convected using a second-order Adams-Bashford scheme with a typical time step of $0.03(W/v_\infty)$, where $v_\infty$ is the upstrem flow velocity. For input to the numerical model, the value for the amplitude of the acoustic particle velocity averaged across the mouth of the resonator tube $u_{\text{mouth}}$ for two different acoustic Strouhal numbers was set to match the analogous water height fluctuation $\Delta h$ at the base of the tube measured by Kawhashi et al.[12] for the same geometry in each case. The relation between these quantities is $\alpha = u_{\text{mouth}}/v_\infty = \Delta h/\Delta h_{\max}$.

#### Interaction of Flow and Sound

The low Mach number form of the wave eqution for acoustic oscillations occuring in an inviscid, isentropic fluid with regions of rotational flow (vortices) is given by[4]

$$\left( \frac{1}{c^2} \frac{\partial^2}{\partial \tau^2} - \nabla^2 \right) B = \nabla \cdot (\omega \times v) \tag{11}$$

where $c$ is the speed of sound, $B$ the stagnation enthalpy, $v$ the fluid velocity, and $\omega = \nabla \times v$ the vorticity. The source term in the wave equation is the Powell dipole $\nabla \cdot (\omega \times v)$. For a given flowfield, Eq. (11) can be solved for the complete acoustic spectrum or for particular Fourier components.

In the present study, the acoustic mode of interest is the resonant field of the resonator tube, which is a solution of Eq. (2) or approximated locally in the neighborhood of the tube mouth by the potential flow solution [see the last term in Eq. (6)]. The energy transferred between the resonant acoustic field and the flowfield can be predicted according to the theory of Howe,[5] who showed that an acoustic power $P$ is generated in a volume $V$ given by

$$P = -\rho_0 \int (\omega \times v) \cdot u \, \mathrm{d}V = -\rho_0 \int \omega \cdot (v \times u) \mathrm{d}V \tag{12}$$

where $u$ is the acoustic particle velocity and $\rho_0$ is the mean density of the fluid. Although vortices will generate sound waves with some spectral components other than the tube resonance, here only the transfer of energy between this dominant resonant mode and the flow is considered. Other nonresonant spectral components will not lead to reflected waves of sufficient amplitude to significantly modify the flow. Once the particular spectral component of interest (in this case the tube resonance) is specified in Eq. (12), then by definition the power $P$ generated by a vortex pertains exclusively to that component.

For a two-dimensional flow, when the vorticity is compact, that is, when the vorticity extends over a region that is small relative to the acoustic wavelength, the acoustic power/unit length of vortex tube generated by a vortex reduces to

$$P = -\rho_0 \Gamma \boldsymbol{k} \cdot (v \times \boldsymbol{u}_o) \sin(2\pi f \tau) \tag{13}$$

where $\Gamma$ is the circulation of the vortex, $\boldsymbol{k}$ the unit vector normal to the plane of the flow, and $\boldsymbol{u}_o$ the amplitude vector of the resonant acoustic particle velocity at the vortex center.

According to Eq. (11), energy transfer between the flowfield and the acoustic field can only take place in those regions where the Coriolis acceleration $(w \times v)$ is nonzero. No exchange of energy between the flow and the acoustic field occurs when the vortex moves parallel to the local acoustic particle velocity, i.e., when $v \times \boldsymbol{u}_o = 0$. Equation (12) also indicates that a nonzero component of the acoustic particle velocity orthogonal to the vortex velocity is required for a nonzero instantaneous acoustic power. Furthermore, for aggregate nonzero acoustic energy to be generated over a sound cycle, variation in at least one of the components of the scalar triple product $\Gamma \boldsymbol{k} \cdot (v \times \boldsymbol{u}_o)$ must occur during this period. For example, near a bluff body, the sound field that a vortex passes through can be modified locally by the presence of the body, leading to a change in $\boldsymbol{u}_o$ and potentially the acoustic power $P$. In the present study, such variation occurs near the trip rod and the walls of the resonator tube.

The concept of acoustic sources and sinks in the present setting needs to be elucidated. First it is noted that the study is focused on the energy transfer between the tube resonant mode and the flowfield. The resonant mode is assumed to have attained its observed equilibrium amplitude. Vortices shed from the trip rod can contribute to the existing resonant acoustic field through wave generation. Whether this contribution is positive or negative depends on the relative phase of the new contribution. If the relative phase is such that the superposition of the newly generated wave adds positively to the existing mode, then the vortex at that stage is classified as a source. That is, the vortex, via the Coriolis acceleration or lifting force $(\omega \times v)$, does work on the resonant acoustic field according to Eq. (12) and energy is transferred from the flowfield. If, however, the new wave is interfering destructively with the existing resonant mode due to its generation being out of phase, then the vortex is deemed to be acting as an acoustic sink. In this case, the resonant acoustic field does work on the flowfield via the lifting force and energy is transferred from the acoustic field to the flowfield. As a vortex translates in space through the time-oscillating and spatially varying resonant sound field, it may alternately act as a source or sink. There will, of course, be other acoustic sinks in the system that are not explicitly determined here, namely, damping mechanisms and transmission losses, which balance the net positive acoustic power generation of the vortices and lead to an equilibrium resonant field.

## Results and Discussion

#### Predicted Resonant Acoustic Field

The predicted acoustic field in the region of the trip rod and the mouth of the resonator tube is shown in Fig. 3. Depicted are the local acoustic particle velocities, which decay rapidly with distance away from the tube opening, at two different phases, representing inflow (penetration) and outflow (evacuation), of the resonant acoustic cycle.

#### Predicted Vortex Shedding

A sequence of snapshots during a vortex shedding cycle is shown in Fig. 4 of the predicted flow when the trip rod is

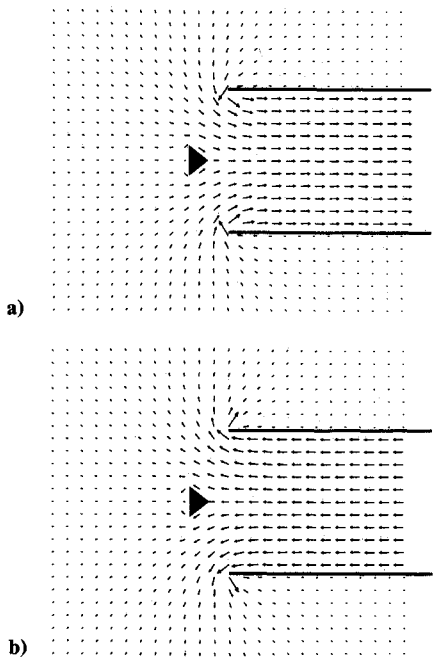


**Fig. 3 Local acoustic particle velocity amplitudes of longitudinal mode of the resonator tube at a) maximum inflow (penetration) and b) maximum outflow (evacuation).**

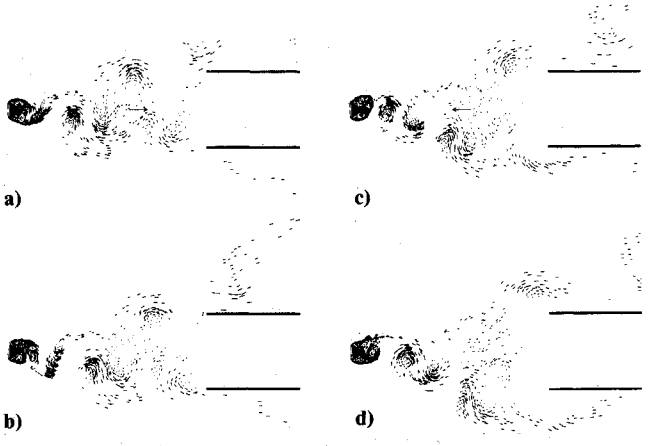


**Fig. 4 Instantaneous plots of elemental vortex positions for the rod placed at $d/W = 5$ at four consecutive phases of acoustic cycle spaced 90-deg apart. The amplitude of the acoustic field was set at $\alpha = 1$.**

placed relatively distant upstream of the tube opening at $d/W = 5$. The vortices are shed from the rod in an asymmetrical manner as for natural Strouhal shedding as observed by Kawahashi et al.,[12] irrespective of the amplitude $\alpha$ of the assumed resonant sound field. In Fig. 4, the extreme case where the sound field is assumed to be at the theoretical maximum value (that is, $\alpha$ is unity) is presented.

The instantaneous acoustic power, normalized by $P_{ref}$, generated in the flow for the rod/tube spacing $d/W = 5$, is shown over a number of consecutive cycles in Fig. 5. The vortex shedding is not correlated by the sound in this case because the amplitude of the acoustic resonant mode decays rapidly away from the opening. At the position of the rod, the amplitude is not large enough to control the vortex shedding. Significant interaction between the vortices and the acoustic field occurs only near the tube opening where the acoustic particle velocity amplitudes can be relatively large. However, because the vortex shedding is not correlated to the assumed resonant acoustic frequency, there is no significant net acoustic energy generated on average. Accordingly, the model predicts that it is not possible for this flow to sustain a loud resonance, which is consistent with the result of Kawahashi et al.[12] who found no tube resonance for this rod/tube spacing.

When the trip rod is placed closer to the resonator tube opening, viz., $d/W = 0.34$, Kawahashi et al.[12] found that the vortex shedding could be modified by the excited acoustic resonance in the tube. For this value of $d/W$, two cases for different acoustic Strouhal number are considered here: 1) $St_a = 0.13$ corresponding to region 2, and 2) $St_a = 0.09$ corresponding to region 3 in Kawahashi et al.[12] (Fig. 6).

**Case 1: $St_a = 0.13$**

Figure 6 shows a sequence of snapshots for the predicted flow when the acoustic Strouhal number is $St_a = 0.13$, using the acoustic amplitude $\alpha = 0.9$ observed in this case by Kawahashi et al.[12] The vortex shedding is quite different for this closer trip rod/tube spacing, being locked to the acoustic resonant frequency and almost symmetrical. During the half-cycle of the acoustic period when the acoustic particle velocities are directed into the tube (Fig. 6a), two new vortices form downstream of the rod. In the next half-cycle when the acoustic particle velocities are directed out of the tube (Fig. 6c), the vortices are shed from the rod and traverse the gap between the rod and the tips of the resonator tube mouth. During this half-cycle, there is also some shedding of vorticity of opposite sign as the flow velocity reverses direction across the leading-edge tips of the wedge. This vorticity collects into secondary

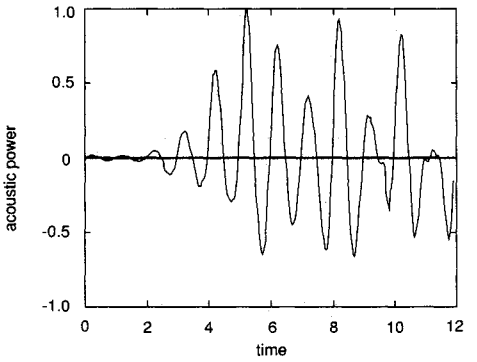


**Fig. 5 Predicted acoustic power output $P$/unit span (scaled to $P_{ref} = \rho v_\infty^3 W/2$) vs time $\tau$ (scaled to acoustic period $T$) for trip rod at $d/W = 5$, $\alpha = 1$.**

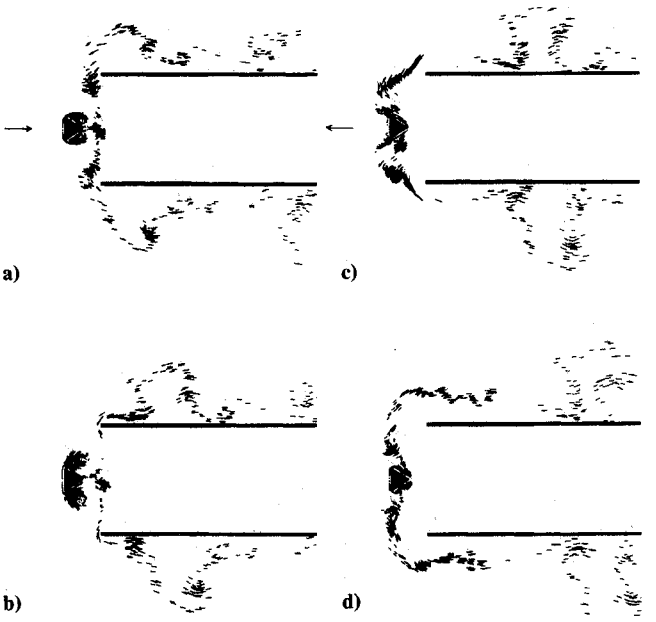


**Fig. 6 Instantaneous plots of elemental vortex positions for the rod placed at $d/W = 0.34$ at four different phases of acoustic cycle, $St_a = 0.13$, $\alpha = 0.9$. The arrow at the left shows the phase of the acoustic cycle.**

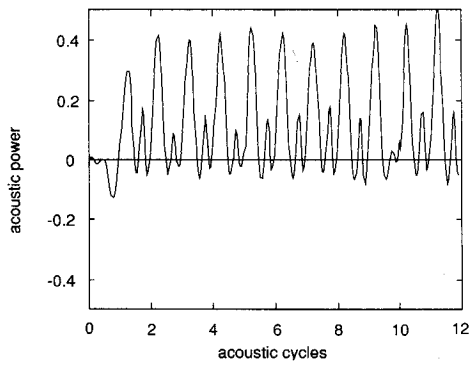


**Fig. 7 Predicted acoustic power output $P$/unit span (scaled to $P_{ref} = \rho_0 v_\infty^3 W/2$) vs time $\tau$ (scaled to acoustic period $T$) for trip rod at $d/W = 0.34$, $\alpha = 0.9$.**

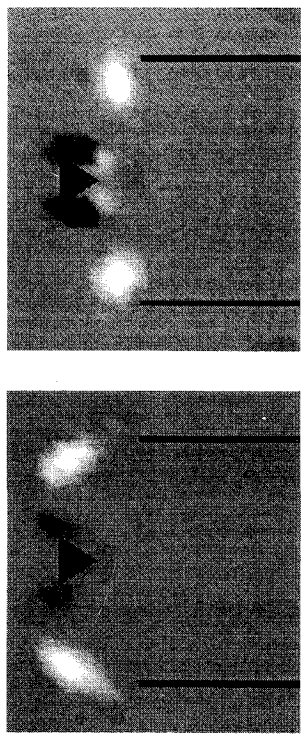

**Fig. 8 Gray scale contours of instantaneous acoustic power generation for trip rod at $d/W = 0.34$ for $St_a = 0.13$ and $\alpha = 0.9$ at a) maximum penetration and b) maximum evacuation. White indicates transfer of energy to the acoustic field and black removal from the acoustic field.**

vortex structures which traverse the gap between the wedge and tube tips during the next inflow phase (Fig. 6a).

The instantaneous acoustic power plot corresponding to the vortex shedding shown in Fig. 6 is shown in Fig. 7. The generation of acoustic power is now quasiperiodic with acoustic energy transferred from the flow to the acoustic field due to the vortices shed from the trip rod during both the inflow and outflow phases. Referring to Fig. 7, the larger peak occurs during the outflow phase and the smaller peak during the inflow phase. The prediction that net acoustic energy per cycle is transferred to the acoustic resonance field is consistent with the measurements of Kawahashi et al.[12]

Gray scale contours of the instantaneous acoustic power given by the Howe formula (12) are shown in Fig. 8 for the same phases of the acoustic cycle as in Figs. 6a and 6c. The individual large-scale vortices shed from the rod can transfer positive (shown as white) or negative (black) acoustic power to the sound field, according to the Howe integral, the sign depending on the phase of the acoustic cycle.

During the formation stage, when the separating shear layers are rolling up and forming large-scale vortex structures near the trailing edge of the trip rod (corresponding to Fig. 6a), Fig. 8a shows that an acoustic source/sink pair is found associated with each structure. Here, the terms source and sink refer to regions where, respectively, positive and negative acoustic power is being generated. Evidently, the sink is considerably more powerful than the source, leading to a transfer of energy from the acoustic field to the flowfield due to these primary vortex structures. This diagram also reveals strong acoustic sources near the tube tips due to secondary vortex structures of opposite circulation that formed during the previous half-cycle when the flow direction across the wedge tips was reversed. The overall result due to both the primary and secondary vortex structures during this (inflow) half-cycle is a net transfer of energy to the acoustic field, as is revealed in Fig. 7.

During the next half-cycle of evacuation from the tube, the primary vortex pair is shed from the trip rod and traverses the mouth of the tube toward the outer tips. At the time of maximum evacuation velocity (corresponding to Fig. 6c), Fig. 8b shows that the large-scale vortices represent a relatively strong acoustic source. The shedding of a pair of secondary vortex structures of opposite circulation is also clearly visible from Fig. 6c. This pair is associated with acoustic sinks during this half-cycle, as depicted in Fig. 8b. The net energy transfer to the acoustic field during the outflow phase is significantly positive.

Contours of the time-average acoustic sources in the flow for $St_a = 0.13$ are shown in Fig. 9. The regions in the vicinity of the tips of the trip rod are time-mean acoustic sinks, and the regions between the rod and the tube tips are distributed time-mean acoustic sources.

### Case 2: $St_a = 0.09$

In this case, the acoustic Strouhal number and the acoustic amplitude ($\alpha = 0.4$) correspond to the region 3 in Kawahashi et al.[12] The trip rod/tube spacing is the same as in case 1. The general flow patterns and the phenomenon of symmetrical shedding (Fig. 10), the predicted acoustic power (Fig. 11), the instantaneous acoustic sources (Fig. 12), and the time-mean acoustic sources (Fig. 13) are similar to those predicted in case

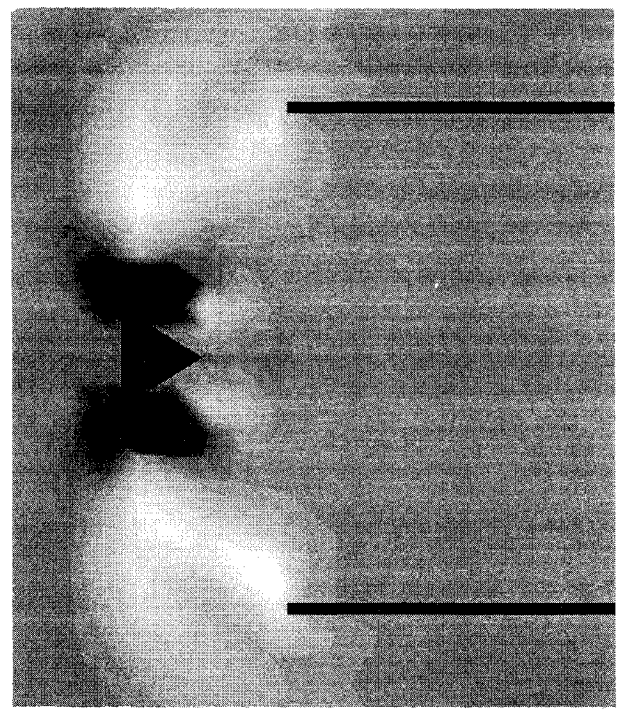

**Fig. 9 Contours of time mean acoustic power generation for trip rod at $d/W = 0.34$ for $St_a = 0.13$, $\alpha = 0.9$.**

1. Positive net energy is predicted per acoustic cycle, which is consistent with the observation of Kawahashi et al.[12] who found the analogy of the acoustic resonance was sustained in this case.

There are, however, some differences between this case and the previous one. With the reduced acoustic field strength, the flow reversal across the leading-edge tips of the trip rod during the outflow phase is not as strong. This means that the secondary vortex structures (clearly visible in Fig. 10d) are very weak and do not contribute significantly to the energy transfer process. Thus, instead of the two peaks per cycle displayed in Fig. 7, there is only one in Fig. 11. This inflow phase results in a net transfer of energy from the acoustic field to the flowfield for this Strouhal number. Because of this, the energy transfer to the acoustic field per cycle is significantly less at this Strouhal number. This is consistent with the observed lower value of the acoustic amplitude in this case.

### Flow in Absence of Acoustic Resonance

In the study by Kawahashi et al.,[12] the vortex shedding pattern was found to change from asymmetric to symmetric as the trip rod was placed progressively closer to the resonator tube. The change in the mode of vortex shedding corresponded to the excitation of the resonant oscillations in the resonator tube. Therefore, it was not clear in their study what the mode of shedding would have been in the absence of resonance excitation.



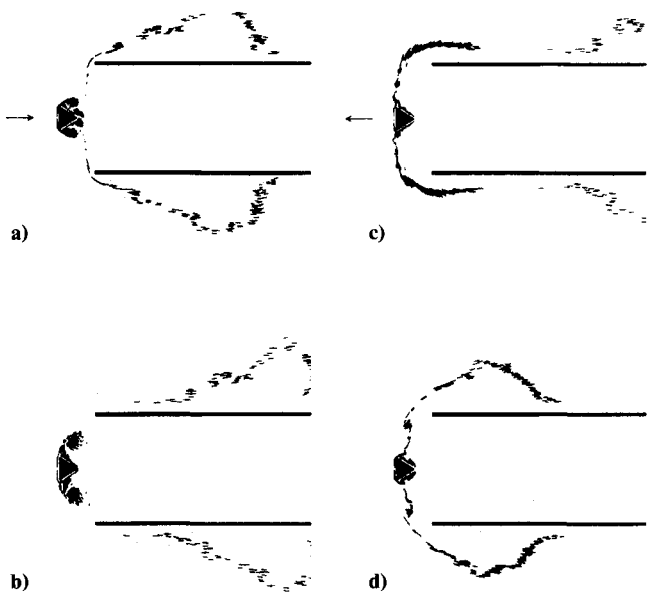


**Fig. 10 Instantaneous plots of elemental vortex positions for the rod placed at $d/W = 0.34$ at four consecutive phases of acoustic cycle, $St_a = 0.09$, $\alpha = 0.4$. The arrow at the left shows the phase of the acoustic field.**

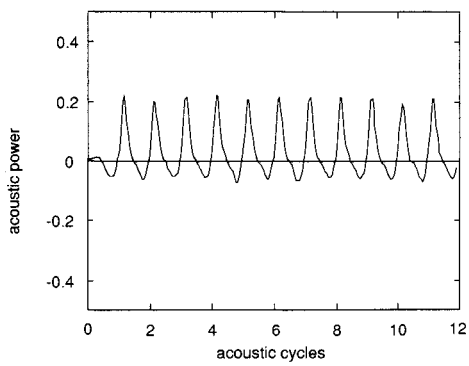


**Fig. 11 Predicted acoustic power output $P$ (scaled to $P_{ref} = \rho_0 v_\infty^3 W/2$) vs time $\tau$ (scaled to acoustic period $T$) for trip rod at $d/W = 0.34$ for $St_a = 0.09$, $\alpha = 0.4$.**

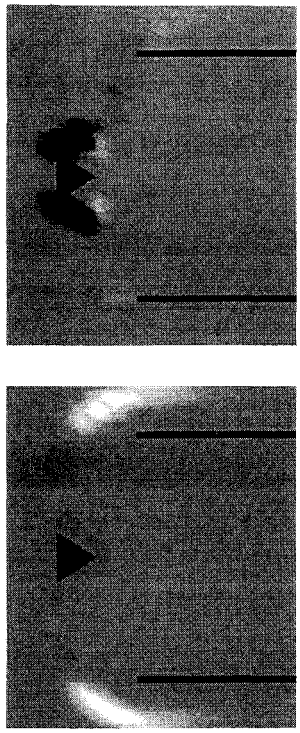

**Fig. 12 Contours of instantaneous acoustic power generation for trip rod at $d/W = 0.34$ for $St_a = 0.09$, $\alpha = 0.4$ at a) maximum penetration and b) maximum evacuation.**

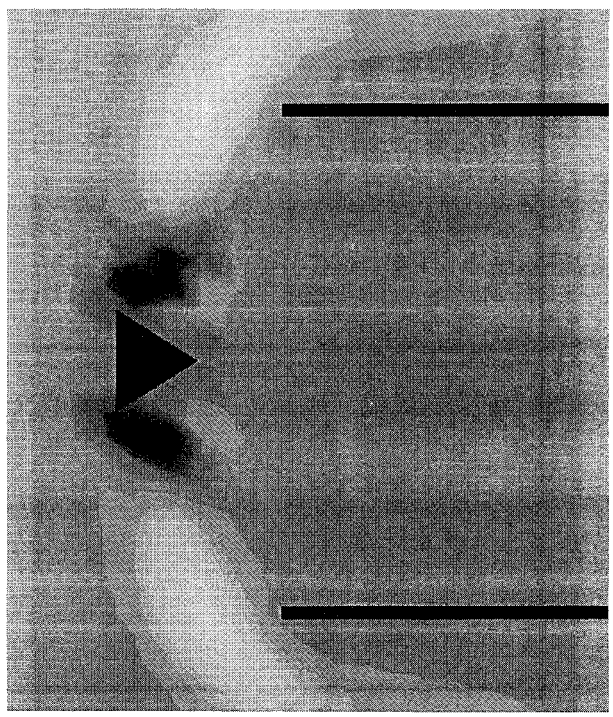

**Fig. 13 Contours of time-mean acoustic power generation for trip rod at $d/W = 0.34$ for $St_a = 0.09$, $\alpha = 0.4$.**

A calculation was performed for the same geometry as in the two previous cases but with the acoustic forcing of the flow suppressed. Snapshots of the flow at different times are shown in Fig. 14. Clearly, when the trip rod is placed sufficiently close to the tube opening, the absolute instability leading to asymmetric Strouhal shedding is suppressed; the two separating shear layers convect to the respective tips of the tube opening with Kelvin-Helmholtz-type instabilities forming in the layers. The effect of exciting the acoustic resonant mode

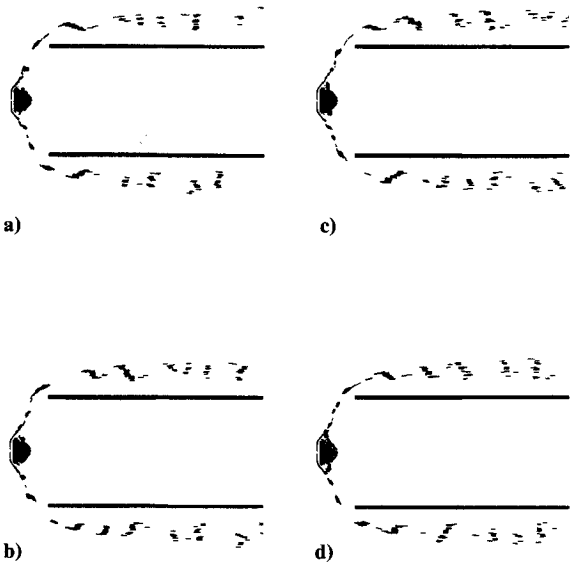


**Fig. 14 Instantaneous plots of elemental vortex positions for rod placed at $d/W = 0.34$ in the absence of a resonant sound field at four consecutive times.**

of the tube is, therefore, the correlating of the convective instabilities in these shear layers with the sound field.

#### Prediction of the Acoustic Sources

According to the theory of Howe[5] and embodied in Eq. (13), a necessary condition for the generation of acoustic power by the flowfield is that vortices must cut across acoustic particle velocity field lines. In the present flow, this can occur to the greatest extent between the trip rod and the opening tips of the resonator tube. This is clear from Fig. 3, which shows the direction of the local acoustic particle velocities, and Figs. 6 and 10, which indicate the movements of the large-scale vortex structures shed from the trip rod for two different acoustic Strouhal numbers. The acoustic particle velocities between the trip rod and the tube mouth possess significant components orthogonal to the paths of the vortices shed from the trip rod, thus allowing a relatively substantial transfer of energy between the flowfield and the resonant acoustic field.

In the case of symmetric shedding, the large-scale vortex structures form along the downstream faces of the trip rod; initially the centroids of the vortices move principally in the longitudinal direction. However, the acoustic particle velocities are modified by the presence of the trip rod and significant vertical components are induced near the rod. During the half sound cycle that the vortices are being formed, the upstream parts of the vortices cut across the acoustic field lines in a manner such that acoustic energy is absorbed from the resonant acoustic field; the downstream portions of the vortices cut across the acoustic field lines with an angle of opposite sign, leading to acoustic source regions. There is, therefore, some cancellation occurring between the sources and sinks, leading to relatively small negative peaks in the instantaneous acoustic power shown in Figs. 7 and 11. In the next half of the sound cycle, the vortices are at full strength, have accelerated, and represent relatively strong acoustic sources with no associated sinks at the time of maximum evacuation from the resonator tube. According to Eq. (13), the positive acoustic power generated during this second half-cycle exceeds the acoustic power absorbed during the first half-cycle. Therefore, the acoustic resonance can be sustained by the net transfer of positive acoustic energy each sound cycle by the vortices moving from the trip rod to the tips of the tube.

Downstream of the tube opening, outside of the tube, the acoustic particle velocities are smaller and are directed almost parallel to the mean flow and the paths of the vortex structures. That is, $v \times u_o$ is relatively small, resulting in little acoustic power generation in this region according to Eq. (13).

The vortices shed from the trip rod represent sources and sinks of sound that can augment a resonant acoustic mode of the tube if the phasing is correct and the vortex shedding is locked to the sound. This locking is effected by acoustic feedback. The feedback is via a resonance, which means that most of the sound energy that influences vortex shedding at any one time was generated in previous cycles, and has been reflected, usually many times, from the resonator tube termination.

## Concluding Remarks

A numerical model has been developed that successfully predicts the experimentally observed flow and acoustic behavior of a hydraulic analogy of the tripped flow past a resonator tube.[12] Emerging from the study is the identification of the convecting acoustic sources with the large-scale vortices shed from the trip rod and the locking of the vortex shedding with the acoustic field.

This study has concentrated on the flow structures responsible for the generation of acoustic power. Further investigations are underway to examine other factors responsible for acoustic damping, such as radiation losses and absorption due to vortex shedding from the tube tips. It is intended that these studies will explain the differences in the observed acoustic amplitude flow velocity is varied. Furthermore, the influence of trip rod size and shape will be investigated.

## References

[1]Blevins, R. D., "The Effect of Sound on Vortex Shedding from Cylinder," *Journal of Fluid Mechanics,* Vol. 61, 1985, pp. 217-237.

[2]Welsh, M. C., Stokes, A. N., and Parker, R., "Flow-Resonant Sound Interaction in a Duct Containing a Plate: Part I. Semi-circular Leading Edge," *Journal of Sound and Vibration,* Vol. 95, No. 3, 1984, pp. 305-323.

[3]Hourigan, K., Welsh, M. C., Thompson, M. C., and Stokes, A. N., "Aerodynamic Sources of Acoustic Vibration in a Duct with Baffles," *Journal of Fluids and Structures,* Vol. 4, 1990, pp. 345-370.

[4]Howe, M. S., "Contributions to the Theory of Aerodynamic Sound, with Application to Excess Jet Noise and the Theory of the Flute," *Journal of Fluid Mechanics,* Vol. 71, 1975, pp. 625-673.

[5]Howe, M. S., "On the Absorption of Sound by Turbulence," *Journal of Applied Mathematics,* Vol. 32, Pt. 4, 1975, pp. 187-209.

[6]Stoneman, S. A. T., Hourigan, K., Stokes, A. N., and Welsh, M. C., "Resonant Sound Caused by Flow past Two Plates in Tandem in a Duct," *Journal of Fluid Mechanics,* Vol. 192, 1988, pp. 455-484.

[7]Vrebalovich, T. T., "Resonance Tubes in a Supersonic Flow Field," Jet Propulsion Lab., California Inst. of Technology, TR 32-378, Pasadena, CA, July 1962.

[8]Brocher, E., "The Response of a Turbulent Flat Plat Boundary Layer to a Sound Wave Moving in the Upstream Direction," *Flow in Real Fluids,* No. 235, Lecture Notes in Physics, Springer-Verlag, Berlin, 1985, pp. 235-242.

[9]Brocher, E., and Duport, E., "Resonators in a Subsonic Flow Field," AIAA Journal, Vol. 26, No. 5, 1988, pp. 548-555.

[10]Fletcher, N. H., and Thwaites, S., "The Physics of Organ Pipes," *Scientific American,* Vol. 248, No. 1, 1983, pp. 84-93.

[11]Brocher, E., Maresca, C., and Bournay, M. H., "Fluid Dynamics of the Resonance Tube," *Journal of Fluid Mechanics,* Vol. 43, Pt. 2, 1970, pp. 369-384.

[12]Kawahashi, M., Brocher, E., and Collini, P., "Coupling of Vortex Shedding with a Cavity," *Fluid Dynamics Research,* Vol. 3, 1988, pp. 369-375.

[13]Morokovin, M. V., "Recent Insights into Instability and Transition to Turbulence in Open-Flow Systems," AIAA Paper 88-3675, 1988.

[14]Tokumaru, P. T., and Dimotakis, P. E., "Rotary Oscillation Control of a Cylinder Wake," *Journal of Fluid Mechanics,* Vol. 224, 1991, pp. 77-90.

[15]Lewis, R. I., "Surface Vorticity Modelling of Separated Flows from Two-Dimensional Bluff Bodies of Arbitrary Shape," *Journal of Mechanical Engineering Science,* Vol. 23, No. 1, 1981, pp. 1-12.

**This article has been cited by:**


1. Devis Tonon, Avraham Hirschberg, Joachim Golliard, Samir Ziada. 2011. Aeroacoustics of pipe systems with closed branches. *Noise Notes* **10**:3, 27-88. [CrossRef]
2. Devis Tonon, Avraham Hirschberg, Joachim Golliard, Samir Ziada. 2011. Aeroacoustics of pipe systems with closed branches. *International Journal of Aeroacoustics* **10**:2, 201-276. [CrossRef]
3. Ganesh Raman, K. Srinivasan. 2009. The powered resonance tube: From Hartmann's discovery to current active flow control applications. *Progress in Aerospace Sciences* **45**:4-5, 97-123. [CrossRef]
4. M.A. Langthjem, M. Nakano. 2005. A numerical simulation of the hole-tone feedback cycle based on an axisymmetric discrete vortex method and Curle's equation. *Journal of Sound and Vibration* **288**:1-2, 133-176. [CrossRef]
5. B.T. Tan, M.C. Thompson, K. Hourigan. 2003. Sources of acoustic resonance generated by flow around a long rectangular plate in a duct. *Journal of Fluids and Structures* **18**:6, 729-740. [CrossRef]
6. A. Mills, G. Raman, V. KibensOptimization of high frequency actuators for weapons bay noise suppression . [Citation] [PDF] [PDF Plus]
7. Ganesh Raman, Valdis KibensActive flow control using integrated powered resonance tube actuators . [Citation] [PDF] [PDF Plus]